Methods xxx (2013) xxx–xxx

Contents lists available at ScienceDirect

Methods

journal homepage: www.elsevier.com/locate/ymeth

Ultra-sensitive nucleic acids detection with electrical nanosensors based on CMOS-compatible silicon nanowire field-effect transistors

Na Lu [a,1], Anran Gao [a,1], Pengfei Dai [a], Tie Li [a,*], Yi Wang [a], Xiuli Gao [a], Shiping Song [b], Chunhai Fan [b,*], Yuelin Wang [a,*]

[a] State Key Laboratories of Transducer Technology and Science and Technology on Micro-system Laboratory, Shanghai Institute of Microsystem and Information Technology, Chinese Academy of Sciences, Shanghai 200050, China
[b] Laboratory of Physical Biology, Shanghai Institute of Applied Physics, Chinese Academy of Sciences, Shanghai 201800, China

ARTICLE INFO

Article history:
Available online xxxx

Keywords:
Ultra-sensitive
Nucleic acids
Silicon nanowire
CMOS-compatible
Biosensor

ABSTRACT

Silicon nanowire field-effect transistors (SiNW-FETs) have recently emerged as a type of powerful nanoelectronic biosensors due to their ultrahigh sensitivity, selectivity, label-free and real-time detection capabilities. Here, we present a protocol as well as guidelines for detecting DNA with complementary metal oxide semiconductor (CMOS) compatible SiNW-FET sensors. SiNWs with high surface-to-volume ratio and controllable sizes were fabricated with an anisotropic self-stop etching technique. Probe DNA molecules specific for the target DNA were covalently modified onto the surface of the SiNWs. The SiNW-FET nanosensors exhibited an ultrahigh sensitivity for detecting the target DNA as low as 1 fM and good selectivity for discrimination from one-base mismatched DNA.

1. Introduction

Investigations of biosensors are of utmost importance because of their widespread application in biomedical analysis, environmental monitoring, food industry, and battlefield detection of warfare agents [1–4]. Detection of nucleic acids (DNA or RNA molecules) has also received great attention since it plays a significant role in genetic diseases and other applications. In recent years, several nanoscale sensing techniques have been reported for the detection of nucleic acids, including electrochemical sensors [5–10], fluorescent sensors [11–14], colorimetric sensors [15–18], quartz crystal microbalance (QCM)-based sensors [19,20], and surface plasmon resonance (SPR)-based sensors [21,22]. Although there have been advancements with each of these approaches, these biosensors need to be tagged with any signaling groups or nanoparticles, which is time-consuming and not easy to operate. It is urged to develop of label-free, rapid and cost-effective biosensors for nucleic acids analysis.

A typical biosensor is an analytical device consisting of three components-molecule recognition, transducer element, and signal processors. In SiNW-FET device, SiNW acted as field-effect transistors (FETs) and revealed a conductance change in respond to variations in the potential or electric field at the surface of the nanowire. As shown in Fig. 1, a standard SiNW-FET is connected to source (S) and drain (D) electrodes, and the conductance is switched by a gate (G) electrode. For n-type NW-FET device, when the negatively charged molecules (such as DNA) bind onto the SiNW surface, an accumulation of carriers takes place in the NW, leading to an decrease in the current of the FET device. On the contrary, the positively charge analytes would result a depletion of carriers, causing a decrease in the conductance of the FET device.

Silicon nanowires (SiNWs), as one-dimensional nanostructures [23], have exhibited ultrahigh sensitivity and multiplex capability [24] because of their small size and large surface-to-volume ratio [25]. A series of excellent properties, the tunability, the reproducible readout, and chemical surface modification also provide unprecedented opportunities to enable SiNWs to be promising candidates for the development of novel biosensors. In particularly, a sensing modality-direct, label-free, and real-time electrical readout-is extraordinarily attractive for many applications. Therefore, SiNWs have emerged as a powerful tool for ultra-sensitive detection of biological and chemical species [26]. To date, there have been a number of silicon nanowire field-effect transistor

Abbreviations: SiNWs, silicon nanowires; SiNW-FETs, silicon nanowire field-effect transistors; CMOS, complementary metal oxide semiconductor; CVD, chemical vapor deposition; PECVD, plasma enhanced chemical vapor deposition; PCB, printed circuit board; SOI, silicon-on-insulator; TMAH, tetramethylammonium hydroxide; V_{DS}, source/drain voltage; I_{DS}, source/drain current; V_{GS}, gate volotage; APTES, (3-aminopropyl) triethoxysilane; SEM, scanning electron microscopy.

* Corresponding authors. Fax: +86 21 6213 1744 (T. Li), +86 21 3919 4702 (C. Fan), +86 21 6213 1744 (Y. Wang).

E-mail addresses: tli@mail.sim.ac.cn (T. Li), fchh@sinap.ac.cn (C. Fan), ylwang@mail.sim.ac.cn (Y. Wang).

[1] These authors contributed equally to this work.

1046-2023/$ - see front matter © 2013 Elsevier Inc. All rights reserved.
http://dx.doi.org/10.1016/j.ymeth.2013.07.012

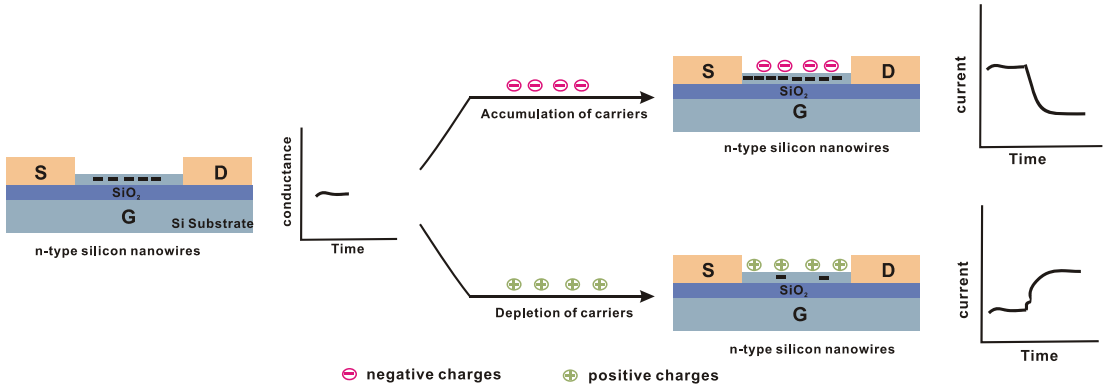

Fig. 1. Schematic of electrical sensing by using n-type FET device. The semiconductor nanowire connected to the source (S) and drain (D) electrodes with a gate (G) electrode on the bottom to modulate the conductance.

(SiNW-FET) nanosensors designed for the detection for various targets, including nucleic acids [27–29], proteins [24,30,31], small-molecules [32], chemical species [26,33], single virus particles [34], and even cells [35,36].

In general, there are two major techniques to fabricate SiNWs: "top-down" and "bottom-up". SiNWs prepared by bottom-up approach [37] are catalytically synthesized by chemical vapor deposition (CVD), which are limited by complex integration due to hybrid fabrication schemes, requiring transfer, low-yield assembly, as well as absence of reliable ohmic contacts. However, the top-down technique [38–40] is based on lithographic processing on a SOI wafer, allowing for the mass production and compatibility with CMOS manufacturing technologies, which is cost-effective and suitable for integration of complex nanowire sensor arrays in different possible applications.

Electrical detection for nucleic acids based upon CMOS-compatible SiNW-FETs is a potential and promising approach. In this report, we present the protocol of fabrication of complementary metal oxide semiconductor (CMOS) compatible SiNWs, which were prepared with an anisotropic wet etching technique with a self-stop limitation. In addition, we also describe the way to surface functionalization of the SiNW with probe DNA, and the application of SiNW-FET nanosensors for detecting nucleic acids. The SiNW-FETs demonstrated ultrahigh sensitivity for DNA detection and excellent discrimination capability for single base pair mismatches.

2. Materials and methods

2.1. Materials

2.1.1. Reagents

Silicon-on-insulator (SOI) wafers (100) (SIMOX)
Photoresist (LC100A)

Buffered hydrofluoric (BHF) acid (Jiangyin Chemical Reagent Factory Co., Ltd.) **!CAUTION** HF is an extremely dangerous material, which is highly corrosive to eyes and skin. Work carefully in the hood with full personal protective equipment.

Tetramethylammonium hydroxide (TMAH; Jiangyin Chemical Reagent Factory Co., Ltd.)
Phosphoric acid, >98% (H_3PO_4; Jiangyin Chemical Reagent Factory Co., Ltd.)

Sulfuric acid, >98% (H_2SO_4; Sinopharm Chemical Reagent Co., Ltd.) **!CAUTION** H_2SO_4 is dangerously corrosive and can cause severe burns.

Hydrogen peroxide, 30% (H_2O_2; Sinopharm Chemical Reagent Co., Ltd.) **!CAUTION** H_2O_2 is an aggressive oxidizer and can cause corrosion.

(3-Aminopropyl) triethoxysilane, ⩾98% (APTES; Sigma–Aldrich)
N-hydroxysuccinimide, ⩾97% (NHS; Fluka)
N-(3-Dimethylamino propyl)-*N*′-ethylcarbodiimide hydrochloride (EDC; Sigma–Aldrich)
Sodium phosphate monobasic, >99% (NaH_2PO4; Sinopharm Chemical Reagent Co., Ltd.)
Sodium phosphate dibasic dodecahydrate, >99% ($Na_2HPO_4 \cdot 12H_2O$; Sinopharm Chemical Reagent Co., Ltd.)
Potassium phosphate dibasic, >99% (KH_2PO_4; Sinopharm Chemical Reagent Co., Ltd.)
Sodium chloride, >99.5% (NaCl; Sinopharm Chemical Reagent Co., Ltd.)
Potassium chloride (KCl; Sinopharm Chemical Reagent Co., Ltd.)
Ethanol, 95% (Sinopharm Chemical Reagent Co., Ltd.)
Milli-Q water (18 MΩ cm; Millipore)

2.1.2. Equipment

Thermal oxidation furnace (4500, Thermco)
Spin-coater (RC8, Suss)
Lithography machine (MA6/BA6, Suss)
Low pressure chemical vapor deposition equipment (LPCVD) (DF550-6, Semco)
Ion beam (I-beam) etcher (Ionfab 300plus, Oxford)
Oxygen plasma cleaner (E300, TePla)
Magnetron sputtering system (Discovery, Denton vacuum)
Plasma-enhanced chemical vapor deposition (PECVD) (Plasmalab system 100, Oxford)
Optical microscopy (STM6, Olympus)
Lithography machine (MA6/BA6, Suss)
Scanning electron microscopy (S4800, Hitachi)
Thermomixer comfort (Eppendorf)
Milli-Q synthesis A10 (Millipore)
Semiconductor property analyzer (4200, Keithley)

2.1.3. Reagent setup

All solutions are prepared with Milli-Q water from a Millipore system.

Phosphate buffer (PB) 10 mM Na_2HPO_4/NaH_2PO_4 (pH ranging from 5.0 to 9.0)

Phosphate buffer solution (1 × PBS) 10 mM Na_2HPO_4 + 2 mM KH_2PO_4 + 37 mM NaCl + 2.7 mM KCl (pH 7.4).

Immobilization buffer (I-buffer) 1 × PBS
Hybridization buffer (H-buffer) 0.1 × PBS
Washing buffer (W-buffer) 0.1 × PBS

2.1.4. Oligonucleotide sequences

All DNA oligonucleotides were custom-synthesized and purified by Shanghai Sangon Bioengineering Technology and Services Co., Ltd. (Shanghai, China), and the sequences as listed in Table 1. Italic base indicates the mismatched one. All DNAs were suspended in Milli-Q water, and stored at −20 °C freezer until experiment.

2.2. SiNW fabrication process

1. Place the SOI wafer into the thermal oxidation furnace at 1000 °C for 119 min. The SiO_2 layer thickness should be 100 nm.
2. Transfer photolithographic pattern onto the surface of SiO_2 by BHF for 30 s.
3. Remove photoresist with oxygen plasma, and etch unprotected Si layer with 25%wt TMAH at 50 °C for 8 min with SiO_2 as mask. The boundary of the active Si layer was automatically aligned to the ⟨110⟩ direction and a very smooth Si(111) plane formed beneath the masking oxide. As a result of the anisotropic wet etching, an angle of 54.74 °C was formed between the (111) and the bottom (100) crystal surface (step a in Fig. 2).
4. Place the cleaned wafer in the chamber of the LPCVD equipment, and deposit a 50 nm thin nitride film on the surface to protect the formed Si(111) plane (step b in Fig. 2).
5. Transfer photolithographic pattern onto the SOI wafer by etching Si_3N_4 with Ionbeam etcher.
6. Remove the SiO_2 layer on the Si by BHF (step c in Fig. 2).
7. Etch the Si(111) planes by using TMAH once again. This step enables homogenous SiNW array with triangular cross-section with self-stop limitation after removing the oxide film (step d in Fig. 2). **CRITICAL STEP** Precisely controlling the etching time is crucial for obtaining a triangular cross-section SiNW with small size.
8. Oxidize the exposed silicon on the wafer surface by thermal oxidation at 950 °C (step e in Fig. 2).
9. Removed all nitride film by 98% phosphoric acid at 150 °C. (step f in Fig. 2).
10. Further thin the SiNW by TMAH at 50 °C for 5 min, to obtain even narrower SiNW with SiO_2 as protected layer after thermal oxide (step g in Fig. 2).

2.3. Equipment setup

Setup of the SiNW-FET device. We define the source/drain electrodes and inner interconnects by photolithography using the photomask, as shown in Fig. 3a. A 600 nm-thick aluminumn (Al) layer was deposited by magnetron sputtering on top of the silicon contact region after removing the SiO_2 from these areas to allow electric contact with Si. Then the sample was annealed at 450 °C for 30 min in nitrogen and hydrogen in order to make reliable ohmic contact between Al and Si, as well as to passivate the interface of the SiNW oxide layer. To enable operation of these devices in an electrolyte solution, we deposited a compact structure of nitride-oxide-nitride stack preventing solution leak by plasma enhanced chemical vapor deposition (PECVD) at 350 °C and the areas of bond pads and nanowire arrays were opened. The fabricated chip was mounted on a testing printed circuit board (PCB) (Fig. 3b). A portable electronic readout system for the use of the SiNW-FET in biosensing experiments was developed. The measurements were performed by using a Keithley 4200 semiconductor parameter analyzer.

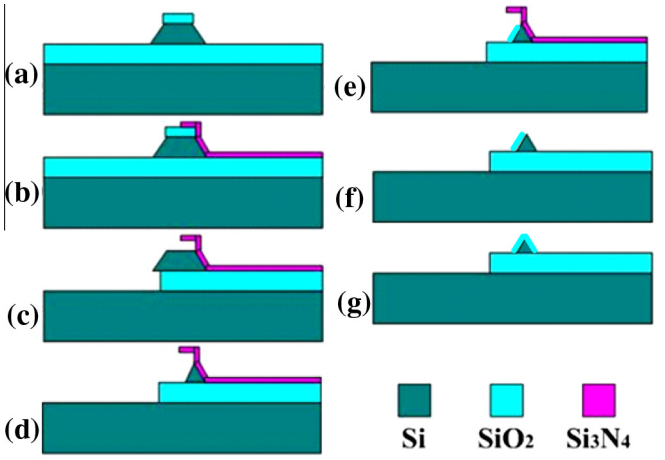

Fig. 2. Schematic illustration of fabrication steps. Reprinted with permission from Ref. [27]. Copyright 2013 American Chemical Society. (a) Anisotropic wet etch unprotected Si layer with TMAH. (b) Deposit a nitride film on the surface to protect Si(111) plane. (c) Remove the SiO2 layer on the Si by BHF. (d) Etch the Si(111) planes by using TMAH once again. (e) Thermally oxidize the exposed silicon on the wafer surface. (f) Removed all nitride film by phosphoric acid. (g) Further thin the SiNW by TMAH to obtain even narrower SiNW.

2.4. Electrical characterization

1. Connect individual SiNW devices on the chip to measure electronics using a Keithley 4200 probe station in combination with a HP semiconductor parameter analyzer (HP 4156 module). Contact probes with the outer metal contact pads on the devices. Measure the curves of current versus voltage by varying gate and source/drain bias voltage to verify the transfer characteristic of the device.
2. For n-type nanowires, measure typical source/drain current versus voltage (I_{DS}/V_{DS}) curves at different gate volotage (V_{GS}) from 0 to + 20 V, in +2 V steps, while V_{DS} varied from 0 to +5 V (Fig. 4a).
3. Monitor the I_{DS}/V_{GS} curves, and sweep V_{GS} from 0 to +20 V, for constant V_{DS} = +1 V. The curves of the SiNW exhibits typical accumulation modulation of n-type devices as the I_{DS} shows saturation with the increase of V_{DS} (Fig. 4b).
4. For p-type nanowires, measure the plots of I_{DS} versus V_{DS} through varying V_{GS} from 0 to −20 V in −2 V steps, while V_{DS} varied from 0 to −5 V (Fig. 4c).

Table 1
Oligonucleotide sequences used in this work.

Oligo DNA	Sequence
Probe DNA	5′-HOOC-CAC GAC GTT GTA AAA CGA CGG CCA G-3′
Target DNA	5′-CTG GCC GTC GTT TTA CAA CGT CGT G-3′
One-base-mismatched DNA	5′-CTG GCC GTC GTT CTA CAA CGT CGT G-3′
Noncomplementary DNA	5′-TGA TAA CCA ATG CAG ATT TTG AGC A-3′

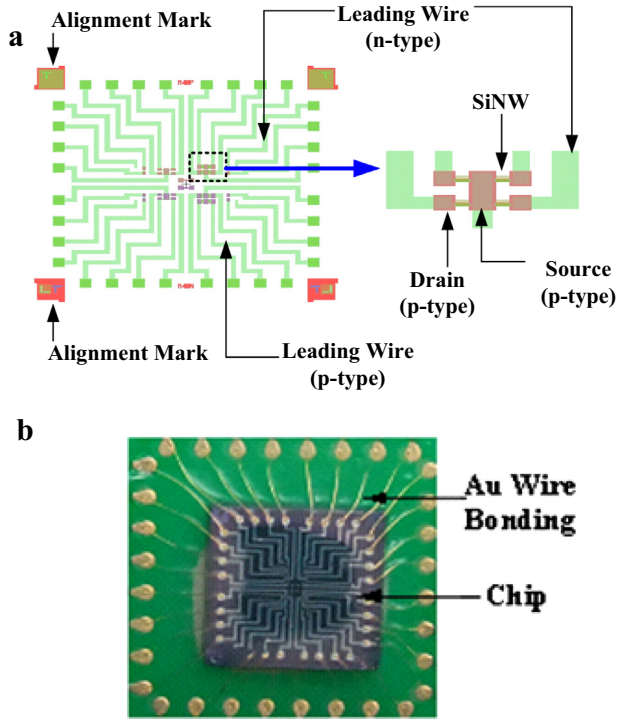

Fig. 3. (a) Photomask design pattern for photolithography. Alignment marks are highlighted with yellow green (p-type) and red colors (n-type), respectively. Thick green lines represent leading wires. In the zoomed image, thin yellow green lines represent SiNWs, thick green lines represent leading wires, wine red stack represent p-type source and drain electrodes with boron adulteration, and purple stacks represent n-type leading wires with phosphorous adulteration. (b) Photo of a prototype SiNW-FET device.

5. The I_{DS}/V_{GS} curve for $V_{DS} = -1$ V was obtained by sweeping the applied voltage V_{GS} from −20 to 0 V. The transfer curves shows typical p-type mode behavior and almost no electronic hysteresis indicating a small density of trapped charges inside the structure (Fig. 4d).
6. From the measurements, select the suitable SiNW devices ready for sensing.

2.5. Surface modification of SiNWs

1. Prepare a piranha solution (98% H_2SO_4/30% H_2O_2, 3:1, v/v), and immerse the cleaned SiNW array chips in the piranha solution at 90 °C for 30 min to remove the contaminations on the surface. Meanwhile, hydroxyl groups were generated terminating the SiO_2 surface, producing a hydrophilic surface.
2. Wash the SiNW array chips with Mill-Q water and absolute ethanol for several times, respectively.
3. Prepare 2% APTES/ethanol solution, and then soak the cleaned SiNW array chips in the solution overnight.
4. Rinse the silanized chips with absolute ethanol for three times to thoroughly remove unreacted APTES, and blow the chips in a stream of nitrogen gas.
5. Incubate the chips in an oven at 120 C and allow to stand for 5 min. A monolayer of self-assembled terminal amines was yielded on the surface.

Note: The silanized surfaces should be used as soon as possible after preparation.

6. Deposit a drop of 1 × PBS buffer solution containing 1 μM of carboxyl-terminated probe DNA, 0.1 M EDC, and 20 mM NHS on the surface of SiNW and allow to react for 2 h at room temperature in a sealed chamber.

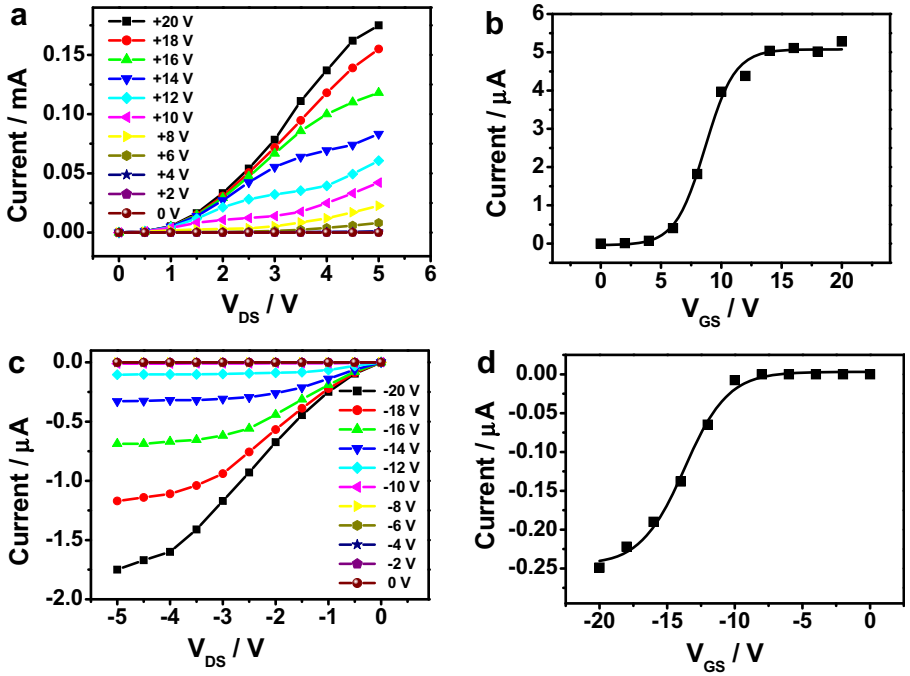

Fig. 4. (a) Plots of I_{SD} versus V_{DS} by varying V_{GS} from 0 to +20 V in +2 V steps. (b) I_{DS} versus V_{GS} curve while $V_{DS} = +1$ V. In (a and b), the used nanowires were n-type, with length of 3 μm. (c) Plots of I_{SD} versus V_{DS} by varying V_{GS} from 0 to −20 V in −2 V steps. (d) I_{DS} versus V_{GS} curve while $V_{DS} = -1$ V. In (c and d), the used nanowires were p-type, with length of 3 μm. Adapted with permission from Ref. [27]. Copyright 2013 American Chemical Society.

7. Wash the surface using 0.1 × PBS buffer solution and Milli-Q water by three times, respectively, and then dry with nitrogen gas. The SiNW array modified with probe DNA were ready for nucleic acid detection.

2.6. Sensing measurements

1. Perform the sensing measurements of SiNW-FET arrays by using the probe station system as described in Section 2.4.
2. Individually connect modified SiNW array chips to probe station, and bring probes into contact with the outer metal contact pads on the chip.
3. Add 0.1 × PBS buffer solution onto the SiNW device, and continuously monitor for tens of seconds until it achieve a stable current. **CRITICAL STEP** It is important to establish a baseline current for each time prior to real-time measurements.
4. Remove the 0.1 × PBS buffer solution, and washed the chips with MillQ-water for three times.
5. Prepare DNA solutions at a series of different concentrations by dissolving 100 μM target species in 0.1 × PBS buffer solution.
6. Add complementary DNA, or noncomplementary DNA, or one-base mismatched DNA in appropriate concentrations (a series of concentrations ranging from fM to nM) onto the surface.
7. Measure the plot of the current versus time and continuously monitor for 100–200 s until a stable current was achieved, which indicates the completion of the binding event.

Note: Real-time measurement for constant V_{DS} = +1 V, V_{GS} = +10 V for n-type SiNWs, and V_{DS} = −1 V, V_{GS} = −12 V for p-type SiNWs, respectively. All devices used for functionalized experiments was similar (w = 200 nm, l = 6 μm) approximately. Each measurement was performed on an individual device. All solutions used in hybridization studies were 0.1 × PBS to ensure effective sensing during the capture process.

2.7. Data analysis

1. The change of current was normalized by computing $|I/I_0|$[31] and plotted on the same axes for the relative change in current of the SiNW device. Here, I represents the value of the final current (t = 100 s), and I_0 represents the value of the initial current (t = 0).
2. In the calibration curve, a relative suppression ratio of the current ($|\Delta I/I_0|$) was defined for the response of the device to the target DNA, where ΔI is the change of the current in the assay.

In this method, there are some most likely problems which users will encounter in Section 2.2–Section 2.6. Therefore, we list them in Table 2 consisting the information of problem, cause, and solution. Please refer to it how to troubleshoot the problems.

3. Results

3.1. SiNW-FET device

To fabricate SiNWs with narrow sizes and high aspect ratios, we developed an anisotropic wet etching approach with self-stop limitation which is compatible with current commercial semiconductor processes or processing. We fabricated the single-crystal SiNWs with diameters ranging from 20 to 200 nm, which have triangular cross section and high surface-to-volume ratio. As illustrated in Fig. 5a, SiNW can be fabricated into a FET device containing source, drain, and gate electrodes. By precisely controlling the etching time and thermal oxidization, the nanowires with the diameter down to 20 nm were obtained (Fig. 5b). The inset of Fig. 5b shows the triangular cross section of the nanowire, with an angle of 54.74° between the top (100) and bottom planes. The cross-section of triangular shape benefits for obtaining so small size of SiNWs, ensuring high sensitivity for sensing. Because of the planarization of the anisotropic wet etching, the surface of the fabricated SiNWs structure was very smooth.

The fabricated SiNW arrays consist of 16 uniform and well-ordered nanowires, as illustrated in Fig. 5c. Such layout of four clusters is suitable for multiplexed detection, as each part may serve as one sensing unit for a particular molecular target. Moreover, the array incorporates both p-type and n-type nanowires on a single chip, allowing effective discrimination of possible electrical cross-talk and false-positive signals by correlating the response versus time from the two types of devices elements. The image of optical microscopy depicts a quarter of SiNW array, in which the NWs are uniform and well-aligned at 70 μm intervals (Fig. 5d). In the chip, each nanowire is electrically addressable by individual insulated metal contact lines.

3.2. Ultra-sensitive detection of DNA

To explore the sensitivity of the SiNW-FET sensor, we measured real-time detection of target DNA with the SiNW-FET sensors. In order to obtain an effective comparison of the relative change in different SiNW devices, the data were normalized by computing $|I/I_0|$ and plotted on the same axes for the relative change, in which, I represents the value of the final current (t = 100 s), and I_0 represents the value of the initial current (t = 0). Fig. 6a illustrated plots of normalized current change ($|I/I_0|$) versus time with the SiNW-FET sensor upon introduction of various concentrations of DNA ranging over 1 fM to 1 nM. Even at the DNA concentration as low

Table 2
Troubleshooting table. The information on how to troubleshoot the most likely problems users will encounter with the method.

Step	Problem	Cause	Solution
2.2 step 7	Uniform fabricated SiNWs	Uncontrolled etching time	Control the etching time by TMAH more precisely
2.2 step 2	SiNWs are broken	Unsmooth lines on photolithographic plate or unproper photolithography	Employ electron beam lithography to fabricate high precision photographic plate. Repeat and optimize photolithography exposure developing conditions
2.4 step 1	Unstable SiNW electrical measurements	Poor electrical contacts	Clean the chip and oxide etching immediately before Al metal deposition, and anneal the chip promptly
2.5 step 6	Solution has dried	Unsealed chamber	Cap the solutions with plastic caps
2.6 step 3	High noisy signal	High nonspecific absorption on the surface of the nanowire	Rinse the probe-modified surface more carefully
2.6 step 7	No signal	Modify the probe DNA in low yield onto the SiNW surface	Use freshly prepared nanowires for DNA sensing assays

Please cite this article in press as: N. Lu et al., Methods (2013), http://dx.doi.org/10.1016/j.ymeth.2013.07.012

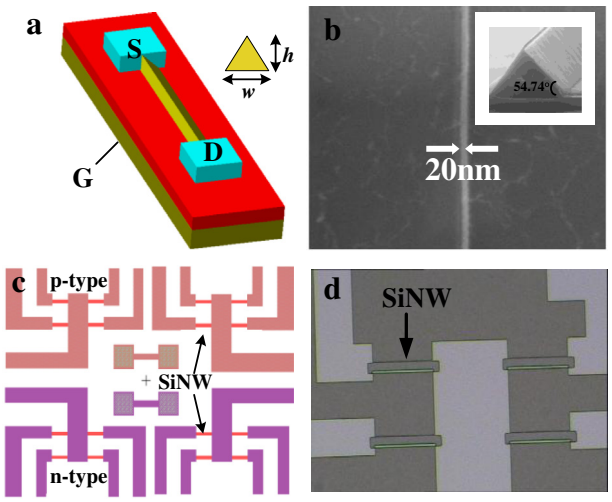

Fig. 5. SiNW-FET device and SiNW array. (a) Schematic illustration of a SiNW-FET device, where S, D and G correspond to source, drain and gate electrode, respectively. Triangle represents the cross-section of SiNW, in which *w* represents the width of SiNW, and *h* represents the height of SiNW. (b) Scanning electron microscopy (SEM) image of a fabricated SiNW with the width less than 20 nm. The inset shows a triangular cross-section, with an angle of 54.74° formed between the Si(1 1 1) and bottom surface. (c) Scheme showing the layout of the SiNW array on the chip. (d) Optical image of a quarter of the SiNW array. Four individual SiNWs are aligned by 70 μm spacing. Adapted with permission from Ref. [27]. Copyright 2013 American Chemical Society.

as 1 fM, a current decrease of ~5% was still observed. A relative suppression ratio of the current ($|\Delta I/I_0|$) was defined for the response of the device to the target DNA in the calibration curve. Here, $\Delta I = I_0 - I$, ΔI is the change of the current in the assay. As demonstrated in Fig. 6b, the relative suppression ratio of the current ($|\Delta I/I_0|$) plotted as a function of the logarithm of DNA concentration. A wide detection range spanning over six orders of concentrations and an ultrahigh sensitivity were achieved for the SiNW devices. The sensitivity is higher than previous reported sensors, possibly resulting from the high surface-to-volume ratio and small size of the SiNW.

We further tested the selectivity of the SiNW sensor. As shown in Fig. 6c, when 100 nM of noncomplementary DNA was introduced, the current demonstrated a negligible change. Upon the addition of 100 nM of fully complementary DNA, a significant decrease of the current was observed, which suggested the binding of target DNA on the n-type SiNW-FET device (seen in Fig. 1). When 1 μM of one-base mismatched DNA was applied on the p-type device, it caused an only change of ~20%, allowing for label-free discrimination between the fully complementary DNA (~50%) and one-base-mismatched DNA (Fig. 6d). This confirmed that the SiNW-FET sensors are capable of single nucleotide polymorphism (SNP) detection which is very important in biomedical research.

4. Discussions

Nucleic acid analysis has also been investigated by other sensing techniques, including electrochemical, fluorescent, and gold nanoparticle-based methods. Compared to these reported approaches, SiNW-FET nanosensor has several significant advantages. Firstly, SiNW-FET has ultrahigh sensitivity owing to their small size and large surface-to-volume ratio, which is potentially utilized in medical point-of-care applications. In addition, it is a label-free method and does not require synthesis and conjugation with nanoparticles, and also the DNA strand does not need to be tagged with any signaling groups (such as fluorophores or chemical groups). Finally, top-down approach could be fabricated of SiNWs in high-yield, which is suitable for mass manufacturing of large scale and compatible with conventional silicon industry. However, SiNW-FET sensors have some limitations in biological measurements, such as the effect of buffer ionic strength on the detection sensitivity. In the long run, we believe that the future is exciting from both science and technology perspectives. We envision that advances in

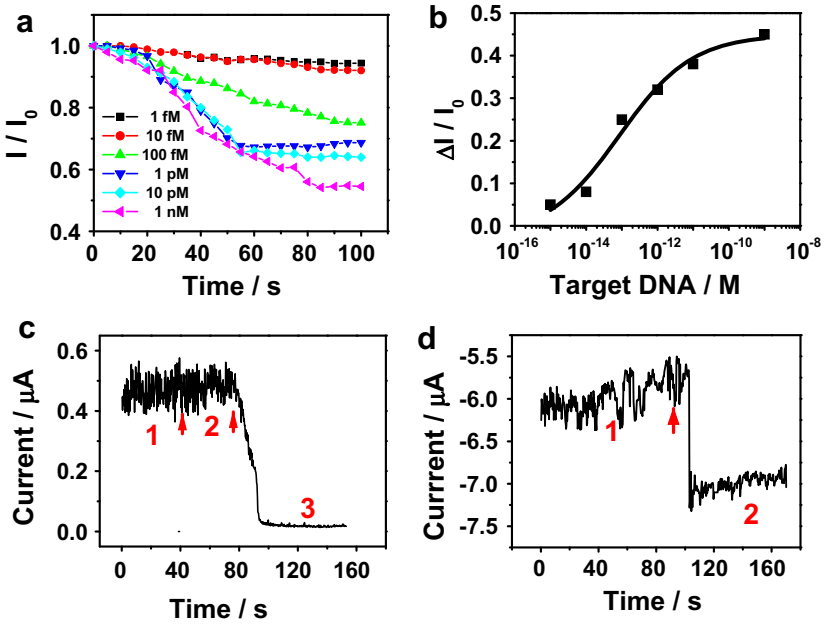

Fig. 6. (a) Plots of normalized current change ($|I/I_0|$) versus time. Concentrations of target DNA in the assay were 1 fM, 10 fM, 100 fM, 1 pM, 10 pM, and 1 nM, respectively. (b) Normalized current change ($\Delta|I/I_0|$) as a function of the logarithm of DNA concentration. (c) Plot of current versus time for modified SiNW-FET device, where region 1 corresponds to buffer solution, region 2 corresponds to the introduction of 100 nM of noncomplementary DNA, and region 3 corresponds to the addition of 100 nM of fully complementary DNA. (d) Plot of current versus time for one-base mismatched detection, where region 1 corresponds to buffer solution, region 2 corresponds to the addition of 1 μM of one-base mismatched sequence. Arrows mark the points when the solutions were introduced. The SiNWs used in (a–c) were n-type, and in (d) were p-type, with length of 6 μm. Reprinted in part with permission from Ref. [27]. Copyright 2013 American Chemical Society.

Please cite this article in press as: N. Lu et al., Methods (2013), http://dx.doi.org/10.1016/j.ymeth.2013.07.012

capabilities of this novel sensor at a commercial level. SiNW-FET would play a significant role in the development for the disease diagnosis, which is important for biomedical applications.

5. Summary

In this report, we described the protocol of an anisotropic wet etching approach for fabricating of CMOS-compatible SiNW arrays and employed SiNW-FET device as an ultra-sensitive biosensor for detecting nucleic acid. Through controlling etching time and the self-limiting oxidation, we obtained homogeneous SiNW arrays with high surface-to-volume ratios and controllable diameters ranging from 20 to 200 nm. The SiNW-FET device demonstrated an label-free, rapid, and real-time electrical DNA sensing and could be detected as low as 1 fM target DNA, which excels previously reported FET-type DNA sensors[38,41–45], as well as with the capability to discriminate from one-base mismatch DNA. In the future, the SiNW-FET sensors may provide a generic platform for numerous applications including point-of care applications.

Competing interest statement

The authors declare no commercial affiliations or financial conflicts of interests in regard to this publication.

Acknowledgements

We appreciate financial support from National Basic Research Program of China (973 Program No. 2012CB933301, No. 2012CB932600), Creative Research of National Natural Science Foundation of China (No. 61021064), the National Natural Science Foundation of China (No. 60936001, No. 91123037, No. 81201358), and the Shanghai International S&T Cooperation Project (No. 12410707300).

References

[1] D. Li, S. Song, C. Fan, Acc. Chem. Res. 43 (2010) 631–641.
[2] J. Wang, Biosens. Bioelectron. 21 (2006) 1887–1892.
[3] S. Song, Y. Qin, Y. He, Q. Huang, C. Fan, H.-Y. Chen, Chem. Soc. Rev. 39 (2010) 4234–4243.
[4] A. Sassolas, B.D. Leca-Bouvier, L.J. Blum, Chem. Rev. 108 (2008) 109–139.
[5] J. Zhang, S. Song, L. Zhang, L. Wang, H. Wu, D. Pan, C. Fan, J. Am. Chem. Soc. 128 (2006) 8575–8580.
[6] G. Liu, Y. Wan, V. Gau, J. Zhang, L. Wang, S. Song, C. Fan, J. Am. Chem. Soc. 130 (2008) 6820–6825.
[7] C.H. Fan, K.W. Plaxco, A.J. Heeger, Proc. Natl. Acad. Sci. USA 100 (2003) 9134–9137.
[8] Y. Xiao, X. Qu, K.W. Plaxco, A.J. Heeger, J. Am. Chem. Soc. 129 (2007) 11896–11897.
[9] J. Wang, G. Liu, A. Merkoci, J. Am. Chem. Soc. 125 (2003) 3214–3215.
[10] H. Pei, N. Lu, Y. Wen, S. Song, Y. Liu, H. Yan, C. Fan, Adv. Mater. 22 (2010) 4754–4758.
[11] S. He, B. Song, D. Li, C. Zhu, W. Qi, Y. Wen, L. Wang, S. Song, H. Fang, C. Fan, Adv. Funct. Mater. 20 (2010) 453–459.
[12] S. Tyagi, D.P. Bratu, F.R. Kramer, Nat. Biotechnol. 16 (1998) 49–53.
[13] J.A.M. Vet, A.R. Majithia, S.A.E. Marras, S. Tyagi, S. Dube, B.J. Poiesz, F.R. Kramer, Proc. Natl. Acad. Sci. USA 96 (1999) 6394–6399.
[14] S. Song, Z. Liang, J. Zhang, L. Wang, G. Li, C. Fan, Angew. Chem- Int. Edit. 48 (2009) 8670–8674.
[15] J. Li, S. Song, X. Liu, L. Wang, D. Pan, Q. Huang, Y. Zhao, C. Fan, Adv. Mater. 20 (2008) 497–500.
[16] W. Xu, X. Xue, T. Li, H. Zeng, X. Liu, Angew. Chem- Int. Edit. 48 (2009) 6849–6852.
[17] F. Xia, X. Zuo, R. Yang, Y. Xiao, D. Kang, A. Vallée-Bélisle, X. Gong, J.D. Yuen, B.B.Y. Hsu, A.J. Heeger, Proc. Natl. Acad. Sci. USA 107 (2010) 10837–10841.
[18] Y. Xiao, V. Pavlov, R. Gill, T. Bourenko, I. Willner, ChemBioChem 5 (2004) 374–379.
[19] F. Caruso, E. Rodda, D.N. Furlong, K. Niikura, Y. Okahata, Anal. Chem. 69 (1997) 2043–2049.
[20] Y. Okahata, Y. Matsunobu, K. Ijiro, M. Mukae, A. Murakami, K. Makino, J. Am. Chem. Soc. 114 (1992) 8299–8300.
[21] L. He, M.D. Musick, S.R. Nicewarner, F.G. Salinas, S.J. Benkovic, M.J. Natan, C.D. Keating, J. Am. Chem. Soc. 122 (2000) 9071–9077.
[22] K.A. Peterlinz, R.M. Georgiadis, T.M. Herne, M.J. Tarlov, J. Am. Chem. Soc. 119 (1997) 3401–3402.
[23] Y.N. Xia, P.D. Yang, Y.G. Sun, Y.Y. Wu, B. Mayers, B. Gates, Y.D. Yin, F. Kim, Y.Q. Yan, Adv. Mater. 15 (2003) 353–389.
[24] G.F. Zheng, F. Patolsky, Y. Cui, W.U. Wang, C.M. Lieber, Nat. Biotechnol. 23 (2005) 1294–1301.
[25] N. Elfstrom, R. Juhasz, I. Sychugov, T. Engfeldt, A.E. Karlstrom, J. Linnros, Nano Lett. 7 (2007) 2608–2612.
[26] Y. Cui, Q.Q. Wei, H.K. Park, C.M. Lieber, Science 293 (2001) 1289–1292.
[27] A. Gao, N. Lu, P. Dai, T. Li, H. Pei, X. Gao, Y. Gong, Y. Wang, C. Fan, Nano Lett. 11 (2011) 3974–3978.
[28] J. Hahm, C.M. Lieber, Nano Lett. 4 (2004) 51–54.
[29] A. Gao, N. Lu, Y. Wang, P. Dai, T. Li, X. Gao, Y. Wang, C. Fan, Nano Lett. 12 (2012) 5262–5268.
[30] E. Stern, J.F. Klemic, D.A. Routenberg, P.N. Wyrembak, D.B. Turner-Evans, A.D. Hamilton, D.A. LaVan, T.M. Fahmy, M.A. Reed, Nature 445 (2007) 519–522.
[31] J.H. Chua, R.-E. Chee, A. Agarwal, S.M. Wong, G.-J. Zhang, Anal. Chem. 81 (2009) 6266–6271.
[32] W.U. Wang, C. Chen, K.H. Lin, Y. Fang, C.M. Lieber, Proc. Natl. Acad. Sci. USA 102 (2005) 3208–3212.
[33] L. Luo, J. Jie, W. Zhang, Z. He, J. Wang, G. Yuan, W. Zhang, L.C.M. Wu, S.-T. Lee, Appl. Phys. Lett. 94 (2009) 193101.
[34] F. Patolsky, G.F. Zheng, O. Hayden, M. Lakadamyali, X.W. Zhuang, C.M. Lieber, Proc. Natl. Acad. Sci. USA 101 (2004) 14017–14022.
[35] T.-S. Pui, A. Agarwal, F. Ye, N. Balasubramanian, P. Chen, Small 5 (2009) 208–212.
[36] X. Duan, R. Gao, P. Xie, T. Cohen-Karni, Q. Qing, H.S. Choe, B. Tian, X. Jiang, C.M. Lieber, Nat. Nanotechnol. 7 (2009) 174–179.
[37] Y. Huang, X.F. Duan, Q.Q. Wei, C.M. Lieber, Science 291 (2001) 630–633.
[38] Z. Li, Y. Chen, X. Li, T.I. Kamins, K. Nauka, R.S. Williams, Nano Lett. 4 (2004) 245–247.
[39] O.H. Elibol, D. Morisette, D. Akin, J.P. Denton, R. Bashir, Appl. Phys. Lett. 83 (2003) 4613–4615.
[40] A. Kim, C.S. Ah, H.Y. Yu, J.-H. Yang, I.-B. Baek, C.-G. Ahn, C.W. Park, M.S. Jun, S. Lee, Appl. Phys. Lett. 91 (2007) 103901.
[41] C.M. Hahm, Lieber, Nano Lett. 4 (2004) 51–54.
[42] Z. Li, B. Rajendran, T.I. Kamins, X. Li, Y. Chen, R.S. Williams, Appl. Phys. A 80 (2005) 1257–1263.
[43] W.C. Maki, N.N. Mishra, E.G. Cameron, B. Filanoski, S.K. Rastogi, G.K. Maki, Biosens. Bioelectron. 23 (2008) 780–787.
[44] C.-H. Lin, C.-H. Hung, C.-Y. Hsiao, H.-C. Lin, F.-H. Ko, Y.-S. Yang, Biosens. Bioelectron. 24 (2009) 3019–3024.
[45] Y.L. Bunimovich, Y.S. Shin, W.-S. Yeo, M. Amori, G. Kwong, J.R. Heath, J. Am. Chem. Soc. 128 (2006) 16323–16331.